

DOA Signal Identification Based on Amplitude and Phase Estimation for Subarray MIMO Radar Applications

Sultan Mahdi, Syahfrizal Tahcfulloh*

*Department of Electrical Engineering
Universitas Borneo Tarakan
Jl. Amal Lama No.1 Tarakan
Tarakan, Indonesia*

Abstract

The overlapped equal subarray transmit radar, which is also known as the Subarray Multiple-Input Multiple-Output radar, utilizes the key advantages simultaneously of both types of multi-antenna radar, i.e., the phased array and MIMO radars, so that it is able to detect multiple targets even though it has a radar cross section (RCS) of a weak or small target. In this paper, it is proposed to develop a parameter estimation approach called amplitude and phase estimation (APES). This approach provides improved resolution to the estimation of the amplitude and direction of arrival (DoA) of the target reflection signal on the radar compared to the existing conventional estimation methods such as least squares (LS). The formulation of the APES method on this radar is based on the tested parameters such as DoA and RCS and continuously being evaluated. The results show that the performance of the APES method of this radar can detect targets very precisely when the number of subarrays (M) is greater than the number of detection targets (P), precisely $M > P$. For the results of DoA and RCS accuracy from the APES method, this radar is more accurate than the LS when testing the angular resolution between the two targets, an angle resolution of 2° is obtained for the APES method which is superior to the LS with an angle resolution of 5.8° . In these conditions, the APES method is able to accurately distinguish between two targets while the LS method is only able to detect one target.

Keywords: amplitude and phase estimation, MIMO, overlapped equal subarray transmit, phased array, radar.

I. INTRODUCTION

Radio detection and ranging, commonly referred to as radar, is a tool that can be used to detect and reach an object through radio waves [1]. The information obtained by the radar comes from the reflected signal such as the distance, number, and velocity of some detected objects. Even if the weather conditions are bad, such as heavy rain, snow, fog, and so on, even at night, the radar is still able to detect the object. Another advantage of radar is that it is able to detect an object at a relatively very far distance, even up to hundreds of kilometers. Therefore, radar is widely implemented in the world of aviation, shipping, and including civil which has a very wide coverage area.

The main functions of radar are detection, parameter estimation, and tracking [1]. However, the very basic function of radar is generally target detection. The detection is a process of identifying the reflected signal received from the intended object or target, or just a noise signal to the receiver (Rx) antenna on the radar [2]. The success of the detection process is closely related to the level of signal to interference plus noise ratio (SINR) on Rx and the ability of the radar to separate the reflected signal from the target and other unwanted reflected sources such as interference and noise. So many approaches have been developed to maximize the SINR

output at Rx and improve the radar's ability to detect signals from the RCS of a small or weak target. One of the radar functions such as parameter estimation is carried out after the detection process occurs, i.e., estimating the range parameters, target velocity, and the direction of arrival (DoA) of the target signal which is estimated based on the reflected signal received. The determination of the waveform plays a major role in the resolution of some of these parameters, such as in research [3] where the non-linear frequency modulation type signal is used on the radar. To achieve the detection of multiple targets, a frequency modulation continuous wave (FMCW) signal can be used as reported in research [4]. Likewise, with the development of the automotive radar, it is necessary to have a radar that has a reliable and high-resolution angle of detection [5]. This paper will focus on the function of this radar, namely parameter estimation, especially related to amplitude and DoA.

The type of radar antenna used in this study is multi-antenna radar with overlapped equal subarray transmit (OEST) which in the research conducted by [6] is known as the phased-MIMO (PMIMO) radar. This radar is a combination of two types of multi-antenna radars, i.e., the phased array (PhA) and the multiple-input multiple-output (MIMO) radars. A hybrid method between the PhA and the MIMO radars has been developed to combine the advantages of the two radar techniques. The OEST radar can be called a MIMO radar with the elements of an overlapped subarray each operating as a PhA. This radar is also designed to combine the advantages of the PhA and the MIMO radars by dividing the transmit (Tx) array into several overlapping subarrays with the same number of antenna elements or with a

* Corresponding Author.

Email: syahfrizal@borneo.ac.id

Received: September 08, 2022 ; Revised: November 03, 2022

Accepted: November 23, 2022 ; Published: December 31, 2022

varying number of elements. The simple concept of this radar is to use a configuration consisting of several subarrays only on the Tx array side. The Tx antenna array can take one of the waveform configurations such as all coherent (commonly used in Tx from PhA radars), non-coherent subarray (commonly used in Tx from MIMO radars), or all noncoherent with the aim of achieving Tx-Rx and high gain SINR. While the Rx side of the array only acts as a non-coherent waveform receiver (commonly used in Rx from MIMO radar).

In the research on parameter estimation, it is proposed to expand the approach called amplitude and phase estimation (APES) for OEST radar where previously the same approach has been carried out for the MIMO radar by [7]-[10]. APES is an adaptive filtering approach referred to as amplitude and phase estimation of a sinusoidal signal for complex spectral estimation. This method can produce a much more accurate spectral estimation where this approach provides a significant resolution improvement to the estimation of the amplitude and DoA of the target reflected signal on the radar compared to conventional estimation methods such as LS [8]. Even in the study by [10], the combination of delay-Doppler-angle parameter estimation methods can be covered well to overcome inter-carrier interference (ICI) on the MIMO-OFDM radar. The advantages of the APES method are also presented in research by [11] regarding spectrum estimation based on synthetic aperture radar (SAR) to improve angular resolution and suppress sidelobe. For the health sector, especially in the cardiovascular system, research by [12] uses APES estimation to track patient blood flow. Thus, the key contributions of this paper that have not been previously reported by other studies [7]-[10] are summarized as follows:

- 1) Formulation and evaluation for APES estimation especially on OEST radar, because in [7]-[10] it is only for the PhA and the MIMO radars.
- 2) Estimation of APES parameters on the proposed radar is considering the effect of the number of targets and subarrays in Tx, comparison with the previous estimation method, and the effect of target angle resolution.

II. PROBLEM FORMULATION AND REVIEW

This research uses OEST type radar with parameter estimation method, namely APES which focuses on observing the ability to detect multiple targets in terms of the number of subarrays in Tx.

A. The OEST Radar

As already stated, the OEST radar is a MIMO radar whose elements are overlapped subarrays with the same number of antenna elements and function as PhA. This radar partitions the Tx array into a number of overlapped subarrays and then each subarray is used coherently to transmit waveforms that are orthogonal to other subarrays.

This radar system can be assumed with co-located antennas as shown in Figure 1 which is composed of U -unit and V -unit elements at Tx and Rx, respectively. The

space between the antenna elements at Tx and Rx is d_U and d_V , respectively. Then the Tx array is formed as many as M -unit subarray whose number of antenna elements per subarray is $U_M = U - M + 1$. The transmitted signal is non-dispersion and narrow-banded. In this radar, the M -unit subarray as an element in the Tx array transmits orthogonal waves simultaneously thereby combining the key advantages of the PhA radar, i.e., directional coherent gain, and the MIMO radar, i.e., the gain of waveform diversity. While the V -unit element of the antenna on the Rx acts as an independent receiver so it can detect multiple targets. On the Tx side of this radar, all waveforms are generated by the signal waveform generator (WG), whose number corresponds to the number of subarrays used, i.e., M . All waveforms per subarray condition the Tx antenna element to radiate into space and its environment to reach the desired targets. Then the targets reflect a signal that depends on the subarray waveform to the radar's Rx antenna. On the Rx side of the radar, the received signal is then processed by the signal processor (SP) through a match filter bank (MFB) according to the waveform emitted from the active subarray.

According to [2], this radar has a virtual array size of MV where M is $1 \leq M \leq U$. The form of the signal received on the OEST radar is expressed by (1).

$$\mathbf{y}(t) = \sqrt{\frac{U}{M}} \sum_{p=1}^P \sigma_p(\theta_p) \mathbf{b}(\theta_p) [\mathbf{c}(\theta_p) \circ \mathbf{d}(\theta_p)]^T \mathbf{x}(t) + \mathbf{n}(t) \quad (1)$$

with coherent and diversity vectors at Tx are $\mathbf{c}(\theta)$ and $\mathbf{d}(\theta)$, respectively, which are represented by (2) and (3).

$$\mathbf{c}(\theta) = [\mathbf{w}_1^H \mathbf{a}_1(\theta) \quad \dots \quad \mathbf{w}_M^H \mathbf{a}_M(\theta)]^T \quad (2)$$

$$\mathbf{d}(\theta) = [e^{-j2\pi f \tau_1(\theta)} \quad \dots \quad e^{-j2\pi f \tau_M(\theta)}]^T \quad (3)$$

where p is the number of targets ($p = 1, 2, \dots, P$), $\sigma(\theta)$ is denoted as the reflection coefficient on the target in the direction θ , $\mathbf{a}(\theta)$ and $\mathbf{b}(\theta)$ are steering vectors at Tx and Rx, \circ is the Hadamard multiplication operator, $(\cdot)^T$ is the transpose operator, $\mathbf{x}(t)$ is the signal waveform which is composed of the waveform $\varphi_m(t)$ for each M -subarrays with $\mathbf{x}(t) = [\varphi_1(t) \quad \varphi_2(t) \quad \dots \quad \varphi_M(t)]^T$, $\mathbf{n}(t)$ is the white zero mean noise vector, $\mathbf{w}_m \in \mathbb{C}^{U \times 1}$ complex weight vector U -unit unit element normal for the m -th subarray, f is the system carrier signal frequency, $\tau_m(\theta)$ is the relative delay time of the first element in the m -th subarray to the first element of the first subarray with $\tau_m(\theta) = kd_U \sin(\theta)/c$, and c is the velocity of light in a vacuum.

B. APES Method on the MIMO Radar

This method is an adaptive filter approach called amplitude and phase estimation of a sinusoidal signal for complex spectral estimation. This method can also produce more accurate spectral estimation [8]. The main contribution to this proposed research is to be able to formulate and evaluate target parameter estimation with

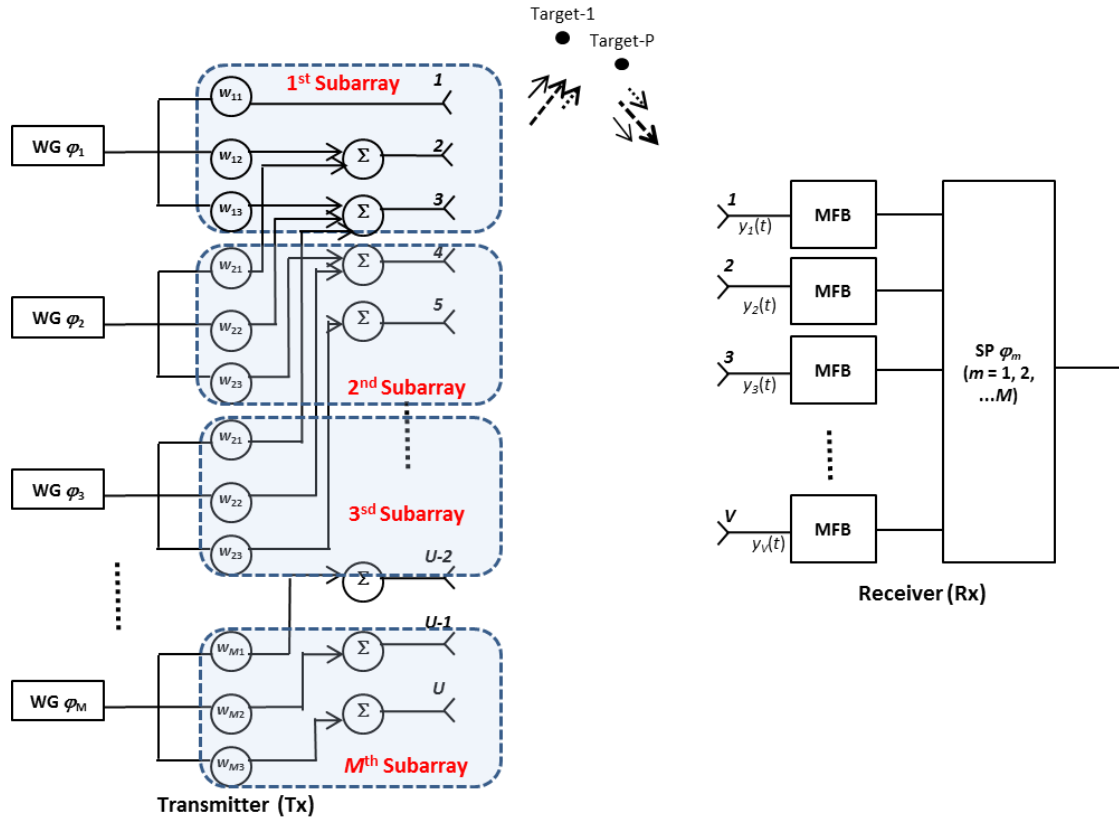


Figure 1. Illustration of the Tx-Rx system of the OEST radar for three antenna elements per subarray.

the APES method which is applied to the OEST radar where this has never been done before including in [7] and [9] for the MIMO radar. Using this method, it is known that the received signal has better accuracy and resolution of amplitude and phase than the conventional method, i.e. LS.

To estimate the number of targets with the APES approach on the MIMO radar is stated by [7], as written in (4).

$$\hat{\sigma}_{MIMO}(\theta) = \frac{\sum_{i=1}^I \mathbf{b}^H(\theta) \hat{\mathbf{Y}}^{-1} \hat{\mathbf{R}}_{\mathbf{y}\mathbf{x}} \mathbf{a}^*(\theta)}{[\mathbf{b}^H(\theta) \hat{\mathbf{Y}}^{-1} \mathbf{b}(\theta)] [\mathbf{a}^T(\theta) \hat{\mathbf{R}}_{\mathbf{x}\mathbf{x}} \mathbf{a}^*(\theta)]} \quad (4)$$

with $\hat{\mathbf{Y}}$ as described in (5).

$$\hat{\mathbf{Y}} = \hat{\mathbf{R}}_{\mathbf{y}\mathbf{y}} - \frac{\hat{\mathbf{R}}_{\mathbf{y}\mathbf{x}} \mathbf{a}^*(\theta) \mathbf{a}^T(\theta) \hat{\mathbf{R}}_{\mathbf{x}\mathbf{y}}}{\mathbf{a}^T(\theta) \hat{\mathbf{R}}_{\mathbf{x}\mathbf{x}} \mathbf{a}^*(\theta)} \quad (5)$$

where $\hat{\sigma}_{AM}(\theta)$ is the estimate of APES on the MIMO radar, i is the number of data samples with $i = 1, 2, \dots, I$, $\hat{\mathbf{R}}_{\mathbf{y}\mathbf{x}}$ is the covariance matrix of the received signal Rx to the waveform, $\hat{\mathbf{R}}_{\mathbf{x}\mathbf{y}}$ is the waveform covariance matrix with respect to the received signal Rx, $\hat{\mathbf{R}}_{\mathbf{x}\mathbf{x}}$ is the auto-covariance matrix of the waveform, $\hat{\mathbf{R}}_{\mathbf{y}\mathbf{y}}$ is the auto-covariance matrix of the received signal Rx, $(\cdot)^H$ is the Hermitian transpose operator, and $(\cdot)^*$ is the transpose conjugate operator.

III. PARAMETER ESTIMATION OF THE RADAR OEST WITH APES METHOD

Estimated target $\hat{\sigma}(\theta)$ which is proportional to the complex amplitude of the echo signal for the LS method turns out to have weaknesses in the form of high sidelobes and low resolution. In conditions where there is strong interference and jamming, the LS method is not able to work effectively. To obtain high resolution target estimates, high amplitude estimation accuracy, and able to suppress interference, the APES method is used. The baseband equivalent signal received by the V -unit antenna element in the Rx array from the proposed radar with the target direction θ_p as in (1). The parameters to be estimated from $\mathbf{y}(t)$ are $\{\sigma_p(\theta_p)\}_{p=1}^P$ and $\{\theta_p\}_{p=1}^P$. If it is assumed that $\mathbf{n}(t)$ and $\mathbf{x}(t)$ are not correlated, the identifiability of the first term of (1) is not affected by the second term at all.

The following are the steps of the APES method used to estimate the number of targets on the proposed radar from (1) which is carried out in stages, i.e.: First is the determination of the APES weight vector $\hat{\mathbf{w}}$ and second is the target estimation $\hat{\sigma}(\theta)$ as in the LS method. The APES method is used as a signal spectrum analyzer [8]. The formulation of the APES method is described by (6).

$$\min_{\mathbf{w}, \sigma} \|\mathbf{w}^H \mathbf{y}(t) - \sum_{p=1}^P \sigma(\theta_p) (\mathbf{c}(\theta_p) \circ \mathbf{d}(\theta_p))^T \mathbf{x}(t)\|^2 \quad (6)$$

subject to $\mathbf{w}^H \mathbf{b}(\theta) = 1$

with the details as written in (7)-(11),

$$\begin{aligned} & \|\mathbf{w}^H \mathbf{y}(t) - \sum_{p=1}^P \sigma(\theta_p) (\mathbf{c}(\theta_p) \circ \mathbf{d}(\theta_p))^T \mathbf{x}(t)\|^2 = \\ & \mathbf{w}^H \hat{\mathbf{R}}_{yy} \mathbf{w} - \sum_{p=1}^P \sigma^*(\theta_p) \mathbf{w}^H \hat{\mathbf{R}}_{yx} (\mathbf{c}(\theta_p) \circ \\ & \mathbf{d}(\theta_p))^* - \sum_{p=1}^P \sigma(\theta_p) (\mathbf{c}(\theta_p) \circ \mathbf{d}(\theta_p))^T \hat{\mathbf{R}}_{xy} \mathbf{w} + \\ & \sum_{p=1}^P \|\sigma(\theta_p)\|^2 (\mathbf{c}(\theta_p) \circ \mathbf{d}(\theta_p))^T \hat{\mathbf{R}}_{xx} \mathbf{a}^*(\theta_p) \end{aligned} \quad (7)$$

where

$$\hat{\mathbf{R}}_{yy} = \frac{1}{I} \sum_{i=1}^I \mathbf{y}(i) \mathbf{y}^H(i) \quad (8)$$

$$\hat{\mathbf{R}}_{yx} = \frac{1}{I} \sum_{i=1}^I \mathbf{y}(i) \mathbf{x}^H(i) \quad (9)$$

$$\hat{\mathbf{R}}_{xy} = \frac{1}{I} \sum_{i=1}^I \mathbf{x}(i) \mathbf{y}^H(i) \quad (10)$$

$$\hat{\mathbf{R}}_{xx} = \frac{1}{I} \sum_{i=1}^I \mathbf{x}(i) \mathbf{x}^H(i) \quad (11)$$

where $\|\sigma(\theta)\|^2 = \sigma(\theta) \sigma^*(\theta)$. The process of (6) aims to obtain a beamformer whose output is similar to the waveform signal, namely $(\mathbf{c}(\theta) \circ \mathbf{d}(\theta))^T \mathbf{x}(t)$. Then minimize (6) which is described in (7) against $\sigma(\theta)$ by looking for the differential in (7) whose result is zero which will become (12).

$$\hat{\sigma}(\theta) = \frac{\sum_{i=1}^I \mathbf{w}^H \hat{\mathbf{R}}_{yx} (\mathbf{c}(\theta) \circ \mathbf{d}(\theta))^*}{(\mathbf{c}(\theta) \circ \mathbf{d}(\theta))^T \hat{\mathbf{R}}_{xx} (\mathbf{c}(\theta) \circ \mathbf{d}(\theta))^*} \quad (12)$$

In (7), it is then minimized with respect to \mathbf{w} using the differential method so as to obtain (13).

$$0 = \mathbf{w}^H \hat{\mathbf{R}}_{yy} - \sum_{p=1}^P \sigma(\theta) (\mathbf{c}(\theta) \circ \mathbf{d}(\theta))^T \hat{\mathbf{R}}_{xy} \quad (13)$$

Then (12) is substituted for (13) resulting in (14) or (15),

$$0 = \mathbf{w}^H \hat{\mathbf{R}}_{yy} - \frac{\sum_{p=1}^P \mathbf{w}^H \hat{\mathbf{R}}_{yx} (\mathbf{c}(\theta) \circ \mathbf{d}(\theta))^* (\mathbf{c}(\theta) \circ \mathbf{d}(\theta))^T \hat{\mathbf{R}}_{xy}}{(\mathbf{c}(\theta) \circ \mathbf{d}(\theta))^T \hat{\mathbf{R}}_{xx} (\mathbf{c}(\theta) \circ \mathbf{d}(\theta))^*} \quad (14)$$

$$0 = \hat{\mathbf{U}} \mathbf{w} = \hat{\mathbf{R}}_{yy} \mathbf{w} - \frac{\sum_{p=1}^P \hat{\mathbf{R}}_{yx} (\mathbf{c}(\theta) \circ \mathbf{d}(\theta))^* (\mathbf{c}(\theta) \circ \mathbf{d}(\theta))^T \hat{\mathbf{R}}_{xy} \mathbf{w}}{(\mathbf{c}(\theta) \circ \mathbf{d}(\theta))^T \hat{\mathbf{R}}_{xx} (\mathbf{c}(\theta) \circ \mathbf{d}(\theta))^*} \quad (15)$$

with $\hat{\mathbf{U}}$ as described in (16).

$$\hat{\mathbf{U}} = \hat{\mathbf{R}}_{yy} - \frac{\hat{\mathbf{R}}_{yx} (\mathbf{c}(\theta) \circ \mathbf{d}(\theta))^* (\mathbf{c}(\theta) \circ \mathbf{d}(\theta))^T \hat{\mathbf{R}}_{xy}}{(\mathbf{c}(\theta) \circ \mathbf{d}(\theta))^T \hat{\mathbf{R}}_{xx} (\mathbf{c}(\theta) \circ \mathbf{d}(\theta))^*} \quad (16)$$

To get the APES weight vector $\hat{\mathbf{w}}$ then at (16) the operation is performed by (17).

$$\min_{\mathbf{w}} \mathbf{w}^H \hat{\mathbf{U}} \mathbf{w} \quad \text{subject to} \quad \mathbf{w}^H \mathbf{b}(\theta) = 1 \quad (17)$$

Furthermore (17) is minimized to \mathbf{w} then produces (18).

$$\hat{\mathbf{w}} = \frac{\hat{\mathbf{U}}^{-1} \mathbf{b}(\theta)}{\mathbf{b}^H(\theta) \hat{\mathbf{U}}^{-1} \mathbf{b}(\theta)} \quad (18)$$

Finally, substitute (18) to (12) to get (19).

$$\hat{\sigma}(\theta) = \frac{\sum_{i=1}^I \mathbf{b}^H(\theta) \hat{\mathbf{U}}^{-1} \hat{\mathbf{R}}_{yx} (\mathbf{c}(\theta) \circ \mathbf{d}(\theta))^*}{[\mathbf{b}^H(\theta) \hat{\mathbf{U}}^{-1} \mathbf{b}(\theta)] [(\mathbf{c}(\theta) \circ \mathbf{d}(\theta))^T \hat{\mathbf{R}}_{xx} (\mathbf{c}(\theta) \circ \mathbf{d}(\theta))^*]} \quad (19)$$

The APES estimation expression for the proposed radar in (19) is the main contribution of this paper. Determination of the form of the formulation is based on the APES estimation of the MIMO radar by [7] and [9] so that (4) can be determined from (19) with the condition that the array Tx is $M = U$ and the array Rx is V so that $\mathbf{a}(\theta) = \mathbf{1}_{U \times 1}$, $\mathbf{d}(\theta) = \mathbf{a}(\theta)$, and $\mathbf{b}(\theta) = \mathbf{1}_{V \times 1}$, consequently at (19) can be simplified to (4), that is described by (20)-(21),

$$\hat{\sigma}(\theta) = \frac{\sum_{i=1}^I \mathbf{b}^H(\theta) \hat{\mathbf{U}}^{-1} \hat{\mathbf{R}}_{yx} \mathbf{a}^*(\theta)}{[\mathbf{b}^H(\theta) \hat{\mathbf{U}}^{-1} \mathbf{b}(\theta)] [\mathbf{a}^T(\theta) \hat{\mathbf{R}}_{xx} \mathbf{a}^*(\theta)]} \quad (20)$$

where

$$\hat{\mathbf{U}} = \hat{\mathbf{R}}_{yy} - \frac{\hat{\mathbf{R}}_{yx} \mathbf{a}^*(\theta) \mathbf{a}^T(\theta) \hat{\mathbf{R}}_{xy}}{\mathbf{a}^T(\theta) \hat{\mathbf{R}}_{xx} \mathbf{a}^*(\theta)} \quad (21)$$

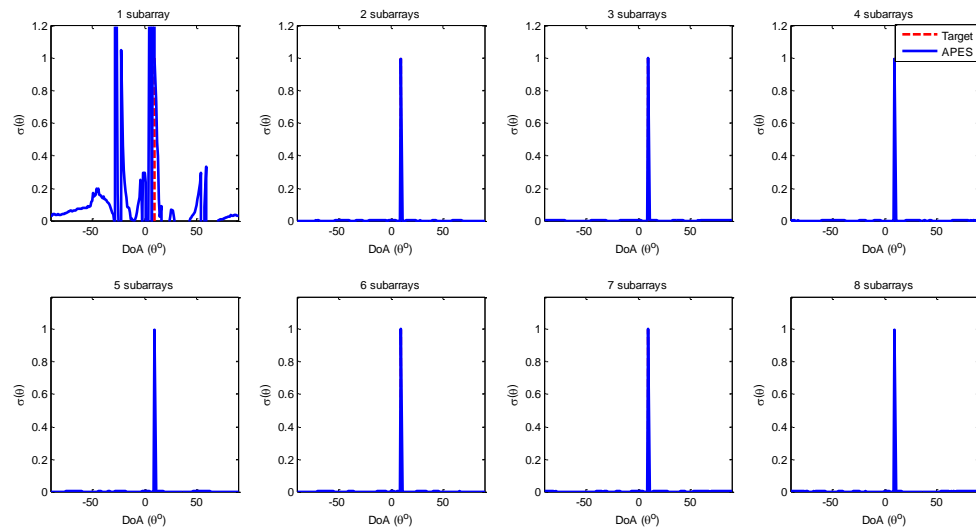
It appears in (20) which is identical to the result in (4) obtained by [7]. Based on this, it can be said that the MIMO radar is a special condition of the OEST radar for $M = U$. Subarray conditions in Tx with $1 \leq M \leq U$ then there will be many conditions from the number of subarrays that emit orthogonal waveform variations to match the conditions of the detected targets, so that it has an impact on the flexibility of target detection capabilities.

IV. RESULTS AND DISCUSSION

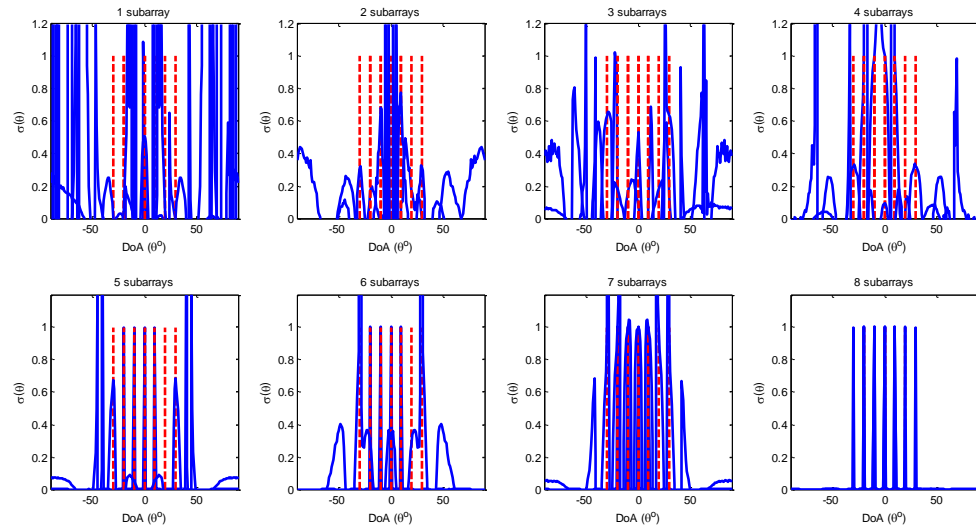
A. APES Estimated Performance on the Radar OEST

It is known in the study by [7] that the APES estimator when applied to the MIMO radar can work well and in different conditions when applied to the PhA radar. This paper does not present a comparison of the performance of the LS and APES estimators which has been presented in detail in [7]. The study presents that the APES estimator is superior to the accuracy and resolution of angle detection and without sidelobe than the LS [7]. So, the focus of this paper is the use of subarray (M) on the proposed radar to the variation in the number of detected targets.

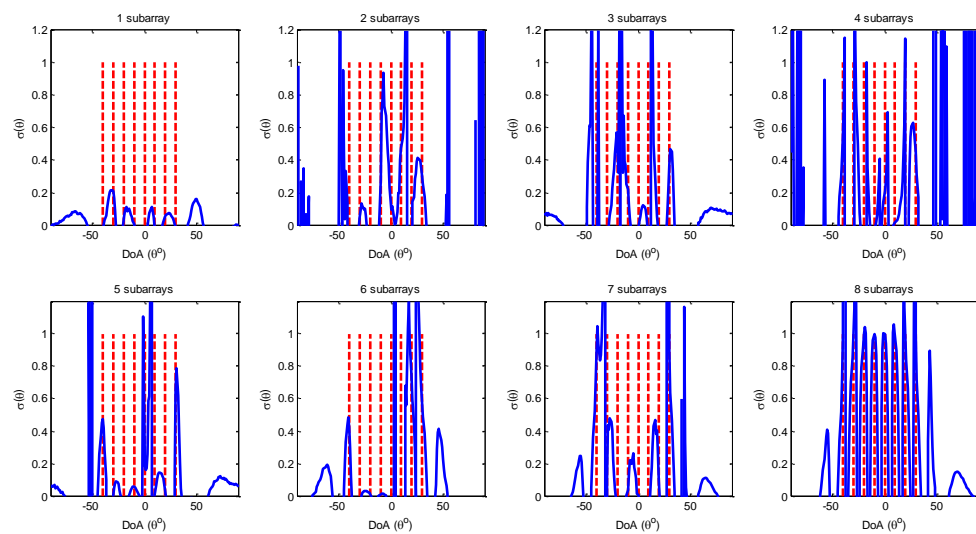
Based on (19) assuming the number of antennas in Tx and Rx from the OEST radar is the same, i.e., $U = V = 8$, where the Tx array has a subarray variation of $1 \leq M \leq U$. The condition of the Tx and Rx antenna spacing, the type of waveform propagation, and the noise properties are in accordance with the study conditions [7].



(a)



(b)



(c)

Figure 2. APES estimator performance on the OEST radar for one to eight subarrays with varying numbers of targets: (a) one target; (b) seven targets; (c) eight targets.

To show the ability of subarray variations on the OEST radar ($1 \leq M \leq 8$), then the performance test of the APES method uses several conditions of the number of targets such as one target, seven targets, and eight targets with $RCS = 1$. Figure 2(a)-(c) is a simulation result of the performance of the APES method for OEST radar. In each simulation result for the desired target detected is given a dotted red line. For the one target condition with DoA (θ) = 10° , Figure 2(a) shows that the proposed radar will detect the given target correctly for a subarray of two to eight. Meanwhile, for this radar with one subarray, one target cannot be detected correctly.

In Figure 2(b) for the case of detecting seven targets, namely DoA (θ) = $\{-30^\circ, -20^\circ, -10^\circ, 0^\circ, 10^\circ, 20^\circ, 30^\circ\}$, only eight subarrays are able to correctly detect the seven targets. Then for the condition of detecting eight targets (see in Figure 2(c)), namely DoA (θ) = $\{-40^\circ, -30^\circ, -20^\circ, -10^\circ, 0^\circ, 10^\circ, 20^\circ, 30^\circ\}$, the APES estimation method on this radar is completely unable to cover the eight targets. So, it can be concluded that the APES estimator can detect targets well when the number of subarrays from the OEST radar is more than the number of targets, or in other words, if the subarray is M and the target is P , the radar will be able to detect the target well when $M > P$. Then when the number of subarrays and targets is the same or $M = P$, then the APES estimator provides a DoA point estimate set with the appropriate RCS of one. This point is not the peak of the mainlobe and there are still errors, thus under these conditions, the estimator can also be considered not able to detect the target correctly.

In addition, Figure 2(a)-(c) indicates that with one subarray it is difficult to detect multiple targets. This happens because to detect one target, a minimum of two subarrays are needed to cover that target. This statement also strengthens the argument in study [7] that the identical PhA radar has one subarray where if this radar applies the APES estimator, then the results are not able to provide target detection as desired.

In OEST radar, when it has one subarray ($M = 1$), then the radar will behave like the PhA radar. In this study, when the subarray $M = 1$, the radar will not be able to detect the target because according to the previous statement that the radar can detect well when the number of subarrays is more than the number of targets. The results of this study also strengthen previous research, namely the use of the APES estimator cannot be used on the PhA radar compiled by [7]. Meanwhile, for the conditions on the OEST radar where the number of antenna elements is U and the number of subarray M with its relation is $M = U$, the OEST radar configuration will be like a MIMO radar. In this study, the OEST radar acts as a MIMO radar when it has a subarray number of $M = 8$ with the ability to detect the maximum number of targets, which is seven targets.

The OEST radar has the advantage of flexibility, which can adjust its subarray according to the number and condition of the detected targets. The use of the APES method on the OEST radar can also be a solution by varying and increasing the number of subarrays where it is known that the APES estimator cannot be configured

as a PhA radar. Another advantage of using the APES estimator on the OEST radar is that the radar can still be conditioned to have a higher coherent gain and can reach a longer detection range, as in the case with the use of two subarrays.

B. Comparative Performance of the APES and LS Methods

To compare the estimation performance between the APES and LS methods on the OEST radar, a condition will be given where the number of subarrays from this radar is set to be greater than the number of targets, namely there are six subarrays to be able to detect four targets which are assumed to be located at $\theta_D = \{-45^\circ, 5^\circ, 15^\circ, 35^\circ\}$, all of which have an RCS of one, as shown in Figure 3. It can be seen in Table 1 that the accuracy of RCS and DoA on the proposed radar for the APES estimator is better than LS using the Root Mean Square Error (RMSE) approach as in research [7]. The APES method has an RMSE for DoA and RCS of 0 while the LS method has RMSE of 1.871 and 0.107, respectively. Table 1 is the result of the RMSE calculation for the accuracy of the RCS and DoA on the LS and APES estimators.

The high RMSE in the LS method is due to the presence of sidelobes which have a high enough level at angles other than those given so that it has an impact on the rise and fall of the mainlobe level. The mainlobes denote the desired target locations whose high and low levels are proportional to the rise and fall of the complex amplitude. The presence of a sidelobe in the estimator results in inaccuracies in DoA detection as stated by [13] that this method has a sidelobe that is sensitive to

TABLE 1
PERFORMANCE COMPARISON OF APES AND LS METHODS WITH
6 SUBARRAYS AND 4 TARGETS θ_D

DoA	RCS	LS		APES	
		DoA	RCS	DoA	RCS
-45°	1	-45°	1.009	-45°	1
5°	1	3°	0.8647	5°	1
15°	1	18°	0.8353	15°	1
35°	1	36°	0.9921	35°	1
RMSE		1.871°	0.107	0°	0

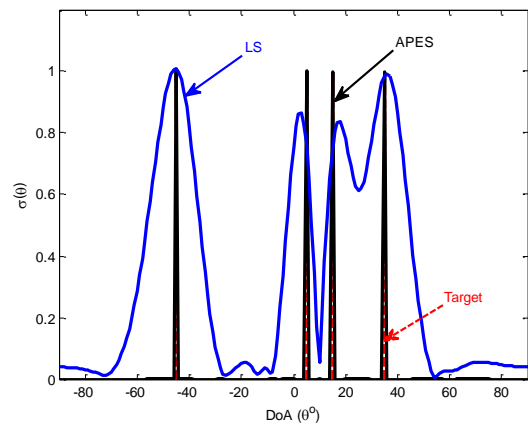


Figure 3. Performance comparison of the APES and LS methods for 6 subarrays, target θ_D , and $RCS = 1$.

triggering interference. Rising and falling mainlobe levels also cause inaccuracies in complex amplitude detection where the value is proportional to the RCS. This is not the case with the APES estimator because this method provides precise resolution of the DoA angle and complex amplitude as has been investigated by [13] for the MIMO radar. The detection accuracy of the APES method is due to the beamforming optimization mechanism by forming a certain weight vector for the signal emitted by the radar [13] where this does not occur in the LS estimator.

To prove the ability of the APES estimator on the OEST radar dealing with unwanted reflected signals such as interference, jammers, etc., an experiment is given as shown in Figure 4. It is known that the APES estimator has almost no sidelobe so that this condition is advantageous when encountering strong interference and jamming. A scenario with three targets located at $\theta_I = \{-35^\circ, -10^\circ, 25^\circ\}$ and all have a complex amplitude of one. A jammer is provided at location 5° with a jammer-to-noise ratio (JNR) of 20 dB. As shown in Figure 4, with the LS estimator, the radar is still affected by the jammer due to the high sidelobe level. Meanwhile, the APES estimator, apart from having very good detection angle resolution, jammer effect is kept to a minimum and there are also no other sidelobes that have the potential to cause other interferences.

C. Impact of RCS Variation

Continuing experiment in Section IV. B, the following experiments are assumed to have the same number of targets, i.e. θ_D but the RCS varies, namely $\{1.5; 0.4; 2.5; 3\}$. This is conditioned to know the ability to estimate complex amplitudes of targets which are indirectly proportional to the RCS of these targets. The varied RCS indicates that there are different targets that have an impact on the ability to reflect the radiation signal back to the radar's Rx antenna. If the target has a small RCS, it indicates that the complex amplitude of the received signal is low and vice versa as stated by [13] where the amplitude is proportional to the RCS.

As shown in Figure 5, the DoA detection ability of the APES method is more accurate than the LS method. This is proven by its ability to detect four target locations where there is one target, namely $\theta = 5^\circ$ of θ_D which is not well covered by LS. Table 2 presents the OEST radar measurement data from the maximum complex amplitude (MCA) for θ_D with varying RCS in both estimators. The RMSE values of the two estimators for MCA on the four targets are 0.09 and 0, respectively. These results also show the superior performance of the APES estimator compared to the LS which supports the results of this study [7].

Figure 5 shows that the APES estimator has the ability to overcome interference due to the minimum sidelobe level other than the desired target location. This is different from the LS estimator where there are several sidelobes whose complex amplitude levels can encourage interference. This is also reinforced by the inability of the LS to detect all given targets.

D. Resolution of the Detection Angle between Two Targets

Angular resolution can be expressed as the difference between two angles which in this study is called DoA of target 1 and target 2, or it can be formulated as follows $\delta_\theta = \theta_1 - \theta_2$, where θ_1 is the position of target 1 and θ_2 is the position of target 2. The smaller the angular resolution, the better the radar's ability to distinguish between two DoA or targets that are close together. If it is assumed that there are two DoA, namely $\theta_1 = 0^\circ$ and $\theta_2 = 2^\circ$, then the angular resolution is 2° with RCS being one. In the case where there are two detected targets, according to the discussion in Section IV. A, when estimating two targets, a minimum number of three subarrays is required. Based on this, an experiment and calculation of angular resolution on the

TABLE 2
COMPARISON OF OEST RADAR AMPLITUDE DETECTION PERFORMANCE WITH RCS VARIATIONS FOR APES AND LS METHODS

Target ($^\circ$)	RCS	LS	APES
-45	1.5	1.51	1.50
5	0.4	0.29	0.40
15	2.5	2.37	2.50
35	3.0	2.97	3.00
RMSE		0.09	0

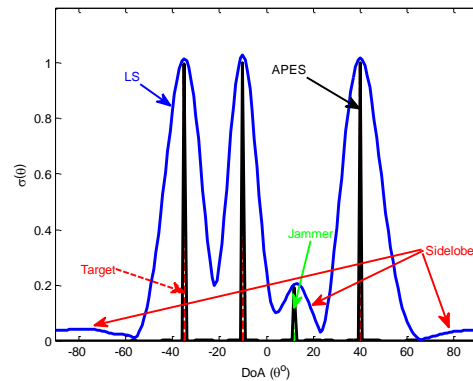


Figure 4. The complex amplitude of the LS and APES methods on the OEST radar for the θ_I and jammer.

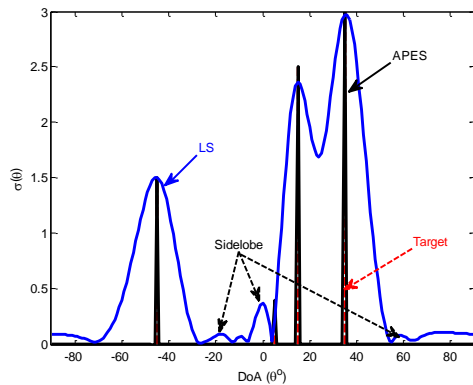


Figure 5. The complex amplitude of the LS and APES methods on the OEST radar for the θ_D and RCS varies targets.

proposed radar as an example with the number of subarrays, i.e., three and eight, were carried out with the aim of comparing the detection performance between the APES and LS methods as shown in Figure 5. In the case of eight subarrays, this is a special condition as a MIMO radar.

Figure 6(a)-(b) shows that the LS estimator is not able to distinguish two targets with a low angular resolution of 2° where the LS estimator can only cover one target with a very high RCS error where it is known according to [7] that the angular resolution is 5.8° . Even the angular resolution results of the OEST radar are still superior compared to the application of the same method to the MIMO radar studied by [7] with an angular resolution of around 3° . This confirms that the use of subarrays in Tx increases the angular resolution of a target detection radar.

The more subarrays from the radar, the smaller the RCS error and so will the sidelobe. In Figure 6(a) with four subarrays, the estimated RCS value of the mainlobe for the LS method is 1.922 and the maximum sidelobe level is 0.274. Meanwhile in Figure 6(b) with eight subarrays, the estimated RCS is 1.825 and the maximum sidelobe level is 0.093. Unlike the LS estimator, the APES estimator is able to distinguish the two targets with a low angular resolution of about 2° where the higher the number of subarrays, the better the angular resolution. There is no sidelobe in the APES estimator as happened in the LS. Besides that, the APES estimator on the OEST

radar is also able to detect targets with the right RCS for the number of subarrays from three to eight. If the number of antenna elements in Tx exceeds eight elements so that each subarray is possible to have many elements, the angular resolution of the proposed method has the potential to be smaller than 2° as to meet the needs of radar angle resolution in automotive radar applications at least around 0.5° [14].

IV. CONCLUSION

The APES estimator for the OEST radar has been formulated and evaluated where the MIMO and the PhA radars are special configurations of the radar. The use of the APES estimator on the proposed radar can detect targets when the number of subarrays is greater than the number of targets. The use of subarrays in Tx increases the angular resolution of a target detection radar. In detecting DoA and RCS, the accuracy of the APES method is better than the LS method where the RMSE of the APES method obtained is 0, while the LS method has the RMSE of DoA and RCS are 1.871 and 0.107, respectively. The APES method is also superior to the LS method in detecting two adjacent targets or at a high resolution of about 2° where this method is still capable of detecting two targets. The use of the APES method on the proposed radar has the advantage of being able to use the advantages of the PhA radar, i.e. high coherent gain using two or more subarrays. Because the proposed radar has the advantage of being flexible, in the future this radar system can be tested for automatic detection with random targets.

DECLARATIONS

Conflict of Interest

In compiling this paper, the authors have solemnly stated that there are no competing interests.

CRedit Authorship Contribution

Sultan Mahdi: Conceptualization, Methodology, Software, Visualization, Investigation, and Writing - Review & Editing; Syahfrizal Tahcfullloh: Data Curation, Writing - Original Draft, Investigation, Writing - Review & Editing, Supervision, Funding Acquisition

Funding

In all the processes and stages of preparing this paper, the authors do not receive financial support from any party for the research, authorship, and/or publication of this article.

Acknowledgment

This research is fully supported by a discussion group at the Telecommunication Systems Laboratory of the Department of Electrical Engineering at the Faculty of Engineering, University of Borneo Tarakan.

REFERENCES

- [1] M. I. Skolnik, *Introduction to Radar Systems*, 3rd ed., New York, USA: McGraw-Hill, 2001.
- [2] S. Tahcfullloh and M. Hardiwansyah, "Parameter estimation and target detection of phased-MIMO radar using capon estimator," *Jurnal Elektronika dan Telekomunikasi*, vol. 20, no. 2, pp. 60-69, Dec. 2020, doi: 10.14203/jet.v20.60-69.

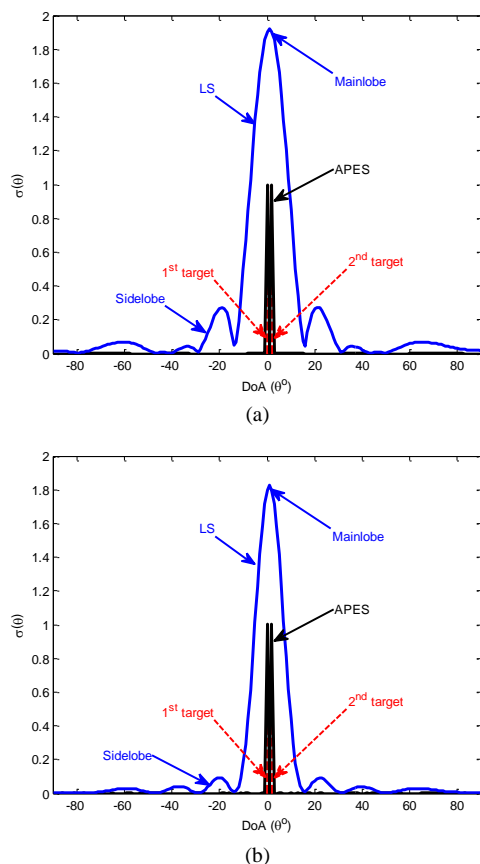


Figure 6. Resolution between two angles in the APES and LS methods: (a) four subarrays; (b) eight subarrays.

- [3] M. R. Widyantara, Sugihartono, F. Y. Suratman, S. Widodo, and P. Daud, "Analysis of non linear frequency modulation (NLFM) waveforms for pulse compression radar," *Jurnal Elektronika dan Telekomunikasi*, vol. 18, no. 1, pp. 27-34, Aug. 2018, doi: 10.14203/jet.v18.27-34.
- [4] H. Pratiwi, M. R. Hidayat, A. A. Pramudita, and F. Y. Suratman, "Improved FMCW radar system for multi-target detection of human respiration vital sign," *Jurnal Elektronika dan Telekomunikasi*, vol. 19, no. 2, pp. 38-44, Dec. 2019, doi: 10.14203/jet.v19.38-44.
- [5] I. Bilik, O. Longman, S. Villeval, and J. Tabrikian, "The rise of radar for autonomous vehicles: signal processing solutions and future research directions," *IEEE Signal Process. Mag.*, vol. 36, no. 5, pp. 20-31, Sep. 2019, doi: 10.1109/MSP.2019.2926573.
- [6] A. Hassanien and S. A. Vorobyov, "Phased-MIMO radar: a tradeoff between phased-array and MIMO radars," *IEEE Trans. Signal Process.*, vol. 58, no. 6, pp. 3137-3151, Jun. 2010, doi: 10.1109/TSP.2010.2043976.
- [7] S. Sapriansa and S. Tahcfullloh, "Identifikasi amplitudo dan sudut kedatangan sinyal menggunakan metode forward-backward APES pada radar multi-antena," *Jurnal Telekomunikasi, Elektronika, Komputasi dan Kontrol*, vol. 7, no. 2, pp. 89-99, Dec. 2021, doi: 10.15575/telka.v7n2.89-99.
- [8] P. Stoica, H. Li, and J. Li, "New derivation of the APES filter," *IEEE Signal Process. Lett.*, vol. 6, no. 8, pp. 205-206, Aug. 1999, doi: 10.1109/97.774866.
- [9] C. Gao, H. Zhou, R. Wu, X. Xu, F. Shen, and Z. Guo, "Parameter estimation and multi-pulse target detection of MIMO radar," in *Proc. 2016 IEEE Region 10 Conf.*, Singapore, Nov. 2016, pp. 909-914, doi: 10.1109/TENCON.2016.7848137.
- [10] M. F. Keskin, H. Wymeersch, and V. Koivunen, "ICI-aware parameter estimation for MIMO-OFDM radar via APES spatial filtering," in *Proc. 2021 IEEE Int. Conf. Acoust. Speech and Signal Process.*, Toronto, Canada, Jun. 2021, pp. 8248-8252, doi: 10.1109/ICASSP39728.2021.9414537.
- [11] H. Zhang and P. López-Dekker, "Persistent scatterer densification through the application of capon- and APES-based SAR reprocessing algorithms," *IEEE Trans. Geosci. Remote Sens.*, vol. 57, no. 10, pp. 7521-7533, Oct. 2019, doi: 10.1109/TGRS.2019.2913905.
- [12] S. M. M. T. Majd and B. M. Asl, "Adaptive spectral doppler estimation based on the modified amplitude spectrum capon," *IEEE Trans. Ultrason. Ferroelectr. Freq. Control*, vol. 68, no. 5, pp. 1664-1675, May 2021, doi: 10.1109/TUFFC.2020.3044774.
- [13] X. Luzhou, J. Li, and P. Stoica, "Target detection and parameter estimation for MIMO radar systems," *IEEE Trans. Aerosp. and Electron. Syst.*, vol. 44, no. 3, pp. 927-939, Jul. 2008, doi:10.1109/taes.2008.4655353.
- [14] J. Zhao, L. Zou, R. Jiang, X. Wang, and H. Gao, "Hybrid antenna arrays with high angular resolution for 77 GHz automotive radars," *Inst. Electron. Inform. and Commun. Eng. Electron. Express*, vol. 17, no. 2, 2020, Art. no. 20190687, doi: 10.1587/elex.16.20190687.